Phase Transitions and the Critical Properties of the Heisenberg Model on a Body-Centered Cubic Lattice

A. K. Murtazaev[a, b, *], M. K. Ramazanov[a, c], D. R. Kurbanova[a], M. A. Magomedov[a, c], M. K. Badiev[a], and M. K. Mazagaeva[a]

[a] *Institute of Physics, Daghestan Scientific Center, Russian Academy of Sciences, Makhachkala, Russia*
[b] *Daghestan State University, Makhachkala, Russia*
[c] *Daghestan Scientific Center, Russian Academy of Sciences, Makhachkala, Russia*
*e-mail: sheikh77@mail.ru

Abstract—The Monte Carlo replica technique is used to study phase transitions and the thermodynamic and critical properties of the three-dimensional Heisenberg antiferromagnetic model on the body-centered cubic lattice with the inclusion of the interaction of the nearest and the next-nearest neighbors. The studies are performed for the proportions of the values of the exchange interactions of the nearest and the next-nearest neighbors in the range of values of k [0.0, 0.6]. The phase transition character is analyzed based on the histogram method. The overall set of static critical indices is calculated in terms of the theory of the finite-dimensional scaling. It is shown that the class of the critical behavior universality of this model is conserved in the above range of values of k.

1. INTRODUCTION

Studying the phase transitions (PT), and the thermodynamic and critical properties of spin systems with frustrations is a central problem of the physics of condensed media. This is related to the fact that frustrated spin systems have the behavior different from the behavior of corresponding nonfrustrated systems. The cause of such behavior is in the strong degeneracy in a spin subsystem [1–4].

The frustration effects are often studied using models with competing exchange interactions of the nearest and the next-nearest neighbors. The existence of competing exchange interactions in magnetic materials can lead to a wide variety of different magnetic ordered states and PTs between them. In addition, the PT features at various values of the proportion of the exchange interactions between the nearest and the next-nearest neighbors are only known in general terms.

The existence of frustrations is known can lead to a change in the PT character and influence the formation of the universality classes of the critical behavior of spin systems. In addition, the inclusion of the antiferromagnetic interactions of the next-nearest neighbors leads to the appearance of various phases and anomalies of the thermodynamic and critical properties [4–9].

In this work, we use the Monte Carlo (MC) method to study the phase transitions, and the thermodynamic and critical properties of the Heisenberg antiferromagnetic model on a body-centered cubic lattice with the inclusion of the interaction of the nearest and the next-nearest neighbors.
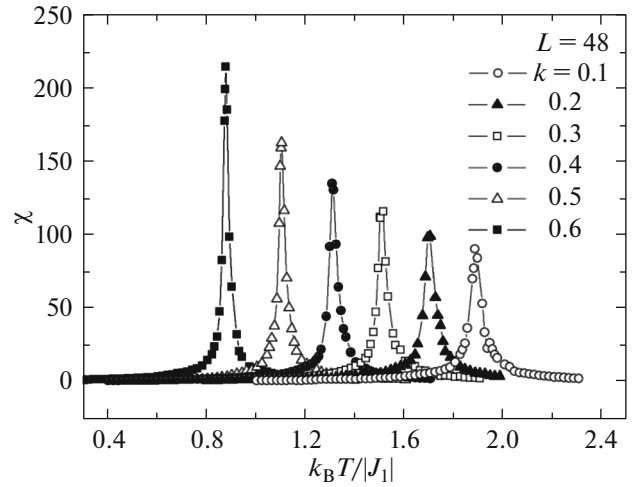
The antiferromagnetic Heisenberg model on the body-centered cubic (bcc) lattice is interesting, since the inclusion of the interactions of the next-nearest neighbors can lead to the appearance of frustrations, which hampers the solution of the problem. Up to now, when studying frustrated systems, the main attention was focused on spin systems on square, triangular, and hexagonal lattices [10–15]. The phase transitions and the critical properties of the frustrated Heisenberg model on a body-centered cubic lattice are only scantly known. In [16], the PTs in this model were studied taking into account the interactions of the nearest and the next-nearest neighbors. The results show that, in this model, the first order PT is observed at the ratio of the exchange interactions of the next-nearest neighbors $k = 1$.

The available data do not enable the unambiguous determination of the PT character and the regularities of changing the critical character of the frustrated Heisenberg model on a bcc lattice at various values of k, and these questions are still open questions.

The study of this model using modern methods and ideas will make it possible to obtain answers a number of questions related to the phase transitions, and the
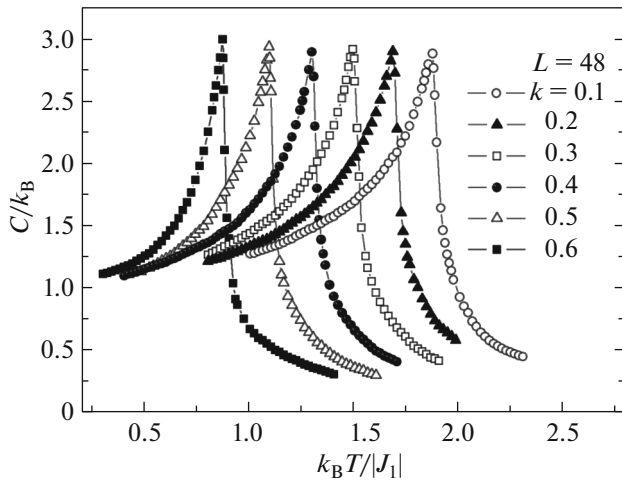
Fig. 1. Heat capacity C/k_B vs. temperature $k_B T/|J_1|$ for $L = 48$ at various k.

Fig. 2. Susceptibility χ vs. temperature $k_B T/|J_1|$ for $L = 48$ at various k.

thermodynamic and critical properties of frustrated spin systems.

2. MODEL AND THE METHOD OF STUDIES

The antiferromagnetic Heisenberg model on a body-centered cubic lattice with allowance for the interactions of the nearest and next-nearest neighbors is described by Hamiltonian

$$H = -J_1 \sum_{\langle i,j \rangle} (\mathbf{S}_i \mathbf{S}_j) - J_2 \sum_{\langle i,l \rangle} (\mathbf{S}_i \mathbf{S}_l), \qquad (1)$$

where $|\mathbf{S}_i|$ is the modulus of three-component unit vector $\mathbf{S}_i = (S_i^x, S_i^y, S_i^z)$. The first term in Eq. (1) takes into account the exchange interaction of the nearest neighbors ($J_1 < 0$), and the second term, the exchange interaction of the next-nearest neighbors ($J_2 < 0$). In our calculation we take $J_1 = 1$ and vary the value of J_2; $k = J_2/J_1$ is the value of the interaction of the next-nearest neighbors. All the parameters are given in the dimensionless form.

The calculations were performed for the systems with periodic boundary conditions and linear sizes $2(L \times L \times L) = N$, $L = 24$–90, where L is measured in the unit cell sizes. The value of the interaction of the next-nearest neighbors was varied within the range k [0.0, 0.6] with a step $\Delta k = 0.1$. To bring the system to the thermodynamic equilibrium state, we cut out a nonequilibrium segment with a length of $\tau_0 = 4 \times 10^5$ MC steps per spin, which is several times larger than the length of the nonequilibrium segment. The averaging of the thermodynamic parameters was carried out along the Markov chain with a length to $\tau = 500\tau_0$ MC step per spin.

The studies of the phase transitions, and the thermodynamic and critical properties of the frustrated

spin systems by the traditional theoretical and experimental methods come up against a number of formidable problems. This is related to the fact that these models are characterized by the problem of numerous valleys of local energy minima. Such systems can be rigorously and successively studied based on microscopic Hamiltonians using the MC methods [10, 12, 14, 16–24], but common MC methods poorly cope with the solution of these problems. Recently, in this connection, many new versions of MC method algorithms that enable one to overcome these problems. Among the most powerful and efficient MC algorithms of the phase transitions and the critical phenomena in the frustrated systems are replica Monte Carlo algorithms [23, 24]. Thus, in this study, we used a high-efficient replica exchange Monte Carlo algorithm.
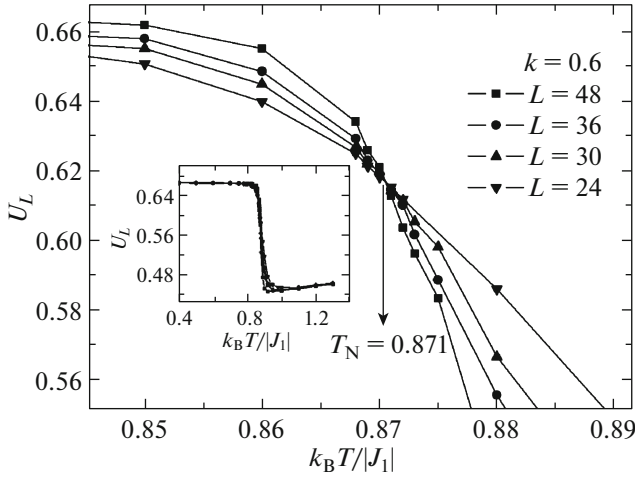
3. RESULTS OF SIMULATION

To observe the temperature dependence of heat capacity C and susceptibility χ, we used the expressions [25, 26]:

$$C = (NK^2)(\langle U^2 \rangle - \langle U \rangle^2), \qquad (2)$$

$$\chi = \begin{cases} (NK)\left(\langle m^2 \rangle - \langle |m| \rangle^2\right), & T < T_N, \\ (NK)\langle m^2 \rangle, & T \geq T_N, \end{cases} \qquad (3)$$

where $K = |J|/k_B T$, N is the number of particles, T_N is the critical temperature (here and below the temperature is given in units of $|J_1|/k_B$, U is the internal energy, and m is the order parameter (U and m are normalized values).

Figures 1 and 2 show the characteristic dependences of the heat capacity and the susceptibility on temperature for the system with linear sizes $L = 48$ at

Fig. 3. Binder commulant U_L vs. temperature $k_B T/|J_1|$ for $k = 0.6$ at various L.

Fig. 4. Histogram of the energy distribution for $k = 0.2$ at $L = 60$ and $L = 90$.

various k (here and in subsequent figures, the statistic error is not larger than the sizes of symbols using for the construction of the dependences).

It is seen from Figs. 1 and 2 that the temperature dependences of heat capacity C and susceptibility χ at all values of k near the critical temperature have pronounced maxima, which shift to lower temperatures as k increases. In this case, an increase in the values of k leads to an increase in the absolute values of the maxima of the susceptibility, which is due to an enhance in fluctuations because of an increase in the competition of the nearest and next-nearest neighbors.

To determine the critical temperature T_N the fourth-order Binder cumulants is most effective [27]:

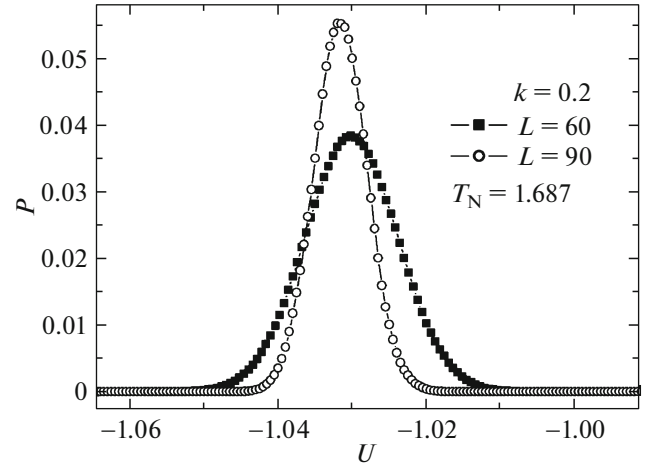$$V_L = 1 - \frac{\langle U^4 \rangle_L}{3 \langle U^2 \rangle_L^2}, \tag{4}$$

$$U_L = 1 - \frac{\langle m^4 \rangle_L}{3 \langle m^2 \rangle_L^2}, \tag{5}$$

where V_L is the energy cumulant and U_L is the magnetic cumulant.

Equation (5) enables one to determine critical temperature T_N at a high accuracy and to test well the PT type in the system.

Figure 3 shows characteristic temperature dependences U_L at $k = 0.6$ for various values of L. It is seen that the clear intersection point ($T_N = 0.871(1)$) is observed in the critical region. By analogy, the critical temperatures were determined also for other values of k.

To analyze the PT order, we also used the histogram analysis of the MC method data [28, 29]. This method allows us to reliably determine the PT order.

The procedure of determining a PT order by this method is described in detail I [30, 31].

Our studies show that PTs for all values k are the second-order transitions. This fact is demonstrated in Figs. 4 and 5, which show the histograms of the distribution of energy for the systems with linear sizes $L = 60$ and $L = 90$ at $k = 0.2$ and $k = 0.6$. The plots were built near the critical temperature. Figures 4 and 5 show that the dependences of probability P on energy U for $k = 0.2$ and $k = 0.6$ have a well-pronounced maximum. The existence of one maximum in the histogram of energy distribution is a sufficient condition of the second-order phase transition. Similar result was obtained also for other values of k.

To calculate the static critical indices of heat capacity α, susceptibility γ, order parameter β, correlation radius ν, and the Fisher index η, we used of the relationships of the finite-dimensional scaling (FDS) theory [32].

From the FDS theory, it follows that, in the system with sizes $L \times L \times L$ at $T = T_N$ and quite large L, the following relationships are fulfilled [32]:
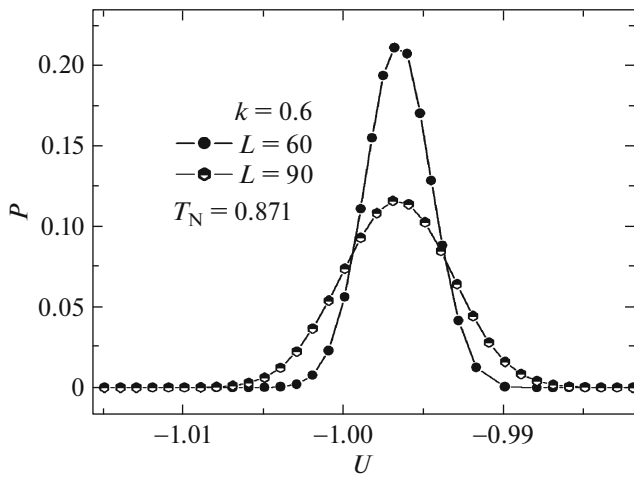
$$m \sim L^{-\beta/\nu}, \tag{6}$$

$$\chi \sim L^{\gamma/\nu}, \tag{7}$$
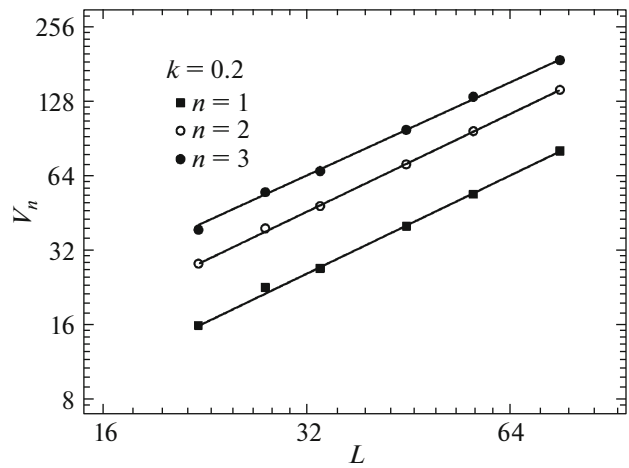
$$V_n \sim L^{1/\nu} g_{V_n}, \tag{8}$$

where g_{V_n} is a constant and V_n can be

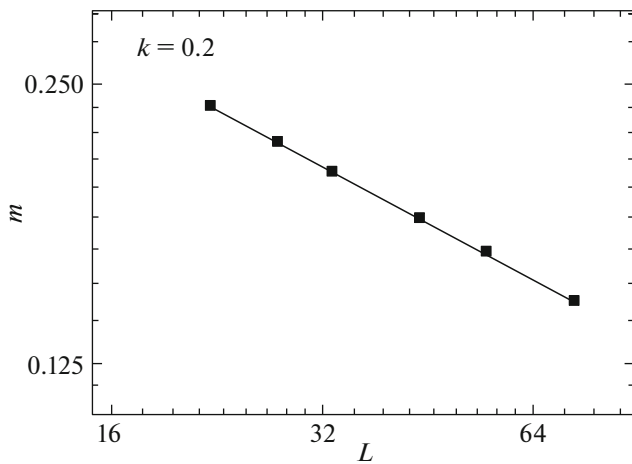$$V_n = \frac{\langle m^n U \rangle}{\langle m^n \rangle} - \langle U \rangle \quad (n = 1, 2, 3). \tag{9}$$

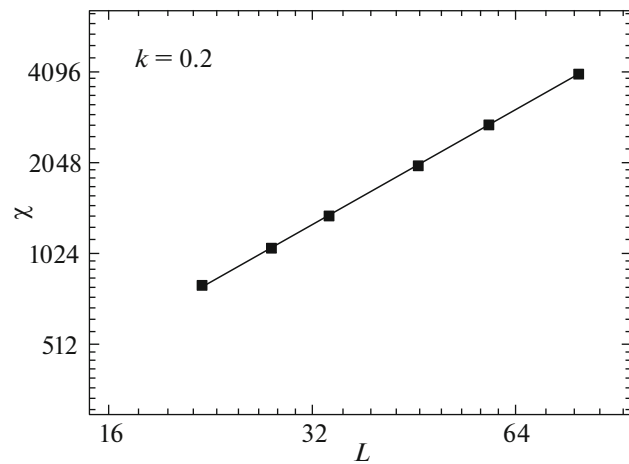These expressions can be used to determine β, γ, and ν.

Fig. 5. Histogram of the energy distribution for $k = 0.6$ at $L = 60$ and $L = 90$.

Fig. 6. Parameter V_n vs. linear sizes of the system L at $T = T_N$ for $k = 0.2$.

Fig. 7. Order parameter m vs. linear sizes of the system L at $T = T_N$ for $k = 0.2$.

Fig. 8. Susceptibility χ vs. linear sizes of the system L at $T = T_N$ for $k = 0.2$.

The temperature dependence of the heat capacity on L, as a rule, the following expression is used

$$C_{\max}(L) = A_1 - A_2 L^{\alpha/\nu}, \qquad (10)$$

where A_1 and A_2 are some coefficients.

Figure 6 shows in a log–log scale shows the characteristic dependences of parameters V_n at $n = 1, 2, 3$ on linear lattice sizes L for $k = 0.2$. As is seen, all the points on the plots well lie on straight lines within the error. The dependence built using the least square technique are parallel to each other. The slope angles of the straight lines determine the value of $1/\nu$. Thus-calculated values of ν were used to determine the critical indices of heat capacity α, susceptibility γ, and order parameter β.

Figures 7 and 8 show in a log–log scale shows the characteristic dependences of magnetic order parameter m and susceptibility χ on linear lattice size L for $k = 0.2$. All the points well lie on straight lines within the error. The slopes of these straight lines determine β/ν and γ/ν. This scheme was used also to determine the values of heat capacity α/ν. Using the data on ν, we calculated static critical indices α, β, and γ.

This procedure was used to calculate the critical indices for all values of k under consideration. The procedure of finding the Fisher index η was described in detail in [33].

All the values of static critical indices obtained in this work are given in Table 1. As is seen from Table 1, almost all values of the critical indices calculated in the range of k [0.0, 0.6] coincide to each other within

Table 1. Critical indices for three-dimensional antiferromagnetic Heisenberg model on a body-centered cubic lattice

k	T_N	ν	α	β	γ	η	$\alpha + 2\beta + \gamma = 2$
0.0	2.056(1)	0.70(1)	−0.13(1)	0.37(1)	1.39(1)	0.02(2)	2.0
0.1	1.873	0.70	−0.12	0.36	1.38	0.03	1.98
0.2	1.687	0.70	−0.13	0.37	1.39	0.02	2.0
0.3	1.494	0.70	−0.12	0.36	1.39	0.02	1.99
0.4	1.301	0.70	−0.12	0.36	1.38	0.03	1.98
0.5	1.094	0.70	−0.12	0.37	1.39	0.02	2.01
0.6	0.871	0.71	−0.13	0.37	1.38	0.03	1.99
Nonfrustrated Heisenberg model [34]	1.443	0.7112(5)	−0.117(2)	0.3689(3)	0.3960(9)	0.0375(5)	2.01

the error. This fact shows that the system demonstrates the universal critical behavior in this range.

Note that the obtained critical indices in the range of k [0.0, 0.6] coincide, within the error, with the corresponding values of the critical indices for the nonfrustrated three-dimensional Heisenberg model [34]. This result shows that, in the above range of k, the inclusion of the interactions of next-nearest neighbors does not lead to a change in the universality class of the critical behavior, and this model belong to the same universality class of the critical behavior as the nonfrustrated three-dimensional Heisenberg model.

4. CONCLUSIONS

The study of the phase transitions, thermodynamic, and critical properties of the three-dimensional antiferromagnetic Ising model on a body-centered cubic lattice with the allowance for the interactions of the nearest and next-nearest neighbors was performed using a high-efficient replica Monte Carlo algorithm. It is shown that, in this model, the second-order phase transition is observed in the range of the interaction of the next-nearest neighbors k [0.0, 0.6]. We calculated all the main static critical indices in this range. It is established that the system demonstrates the universal critical behavior in the noted range of k.

FUNDING

REFERENCES

1. S. S. Sosin, L. A. Prozorova, and A. I. Smirnov, Phys. Usp. **48**, 83 (2005).
2. V. S. Dotsenko, Phys. Usp. **38**, 457 (1995).
3. S. E. Korshunov, Phys. Usp. **49**, 225 (2006).
4. S. V. Maleev, Phys. Usp. **45**, 569 (2002).
5. M. Tisser, B. Delamotte, and D. Mouhanna, Phys. Rev. Lett. **84**, 5208 (2000).
6. P. Calabrese, P. Parruccini, A. Pelissetto, and E. Vicari, Phys. Rev. B **70**, 174439 (2004).
7. G. Zumbach, Nucl. Phys. B **413**, 771 (1994).
8. A. Pelissetto, P. Rossi, and E. Vicari, Phys. Rev. B **63**, 140414(R) (2001).
9. D. P. Landau and K. Binder, *Monte Carlo Simulations in Statistical Physics* (Cambridge Univ. Press, Cambridge, 2000), p. 384.
10. A. K. Murtazaev, M. K. Ramazanov, F. A. Kasan-Ogly, and D. R. Kurbanova, J. Exp. Theor. Phys. **120**, 110 (2015).
11. H. Kawamura, J. Phys. Soc. Jpn. **61**, 1299 (1992).
12. A. Mailhot, M. L. Plumer, and A. Caille, Phys. Rev. B **50**, 6854 (1994).
13. L. E. Svistov, A. I. Smirnov, L. A. Prozorova, O. A Petrenko, A. Ya. Shapiro, and L. N. Dem'yants, JETP Lett. **80**, 204 (2004).
14. A. K. Murtazaev, M. K. Ramazanov, and M. K. Badiev, J. Low Temp. Phys. **37**, 1001 (2011).
15. F. A. Kassan-Ogly, B. N. Filippov, A. K. Murtazaev, M. K. Ramazanov, and M. K. Badiev, J. Magn. Magn. Mater. **324**, 3418 (2012).
16. A. K. Murtazaev, M. K. Ramazanov, D. R. Kurbanova, and M. K. Badiev, Phys. Solid State **60**, 1173 (2018).
17. A. K. Murtazaev, M. K. Ramazanov, and M. K. Badiev, J. Exp. Theor. Phys. **115**, 303 (2012).
18. A. K. Murtazaev, M. K. Ramazanov, and M. K. Badiev, Phys. B: Condens. Matter **476**, 1 (2015).
19. F. A. Kassan-Ogly, A. K. Murtazaev, A. K. Zhuravlev, M. K. Ramazanov, and A. I. Proshkin, J. Magn. Magn. Mater. **384**, 247 (2015).
20. M. K. Ramazanov, A. K. Murtazaev, and M. A. Magomedov, Solid State Commun. **233**, 35 (2016).
21. A. K. Murtazaev, M. K. Ramazanov, M. A. Magomedov, and D. R. Kurbanova, Phys. Solid State **60**, 1848 (2018).
22. A. K. Murtazaev and M. K. Ramazanov, Phys. Solid State **53**, 1067 (2011).
23. A. Mitsutake, Y. Sugita, and Y. Okamoto, Biopolymers (Peptide Sci.) **60**, 96 (2001).
24. A. K. Murtazaev, M. K. Ramazanov, F. A. Kasan-Ogly, and M. K. Badiev, J. Exp. Theor. Phys. **117**, 1091 (2013).

25. K. Binder and J.-Sh. Wang, J. Status Phys. **55**, 87 (1989).

26. P. Peczak, A. M. Ferrenberg, and D. P. Landau, Phys. Rev. B **43**, 6087 (1991).

27. K. Binder and D. Heermann, *Monte Carlo Simulation in Statistical Physics* (Springer, Berlin, 2010).

28. F. Wang and D. P. Landau, Phys. Rev. Lett. **86**, 2050 (2001).

29. F. Wang and D. P. Landau, Phys. Rev. E **64**, 056101 (2001).

30. M. K. Ramazanov and A. K. Murtazaev, JETP Lett. **106**, 86 (2017).

31. M. K. Ramazanov and A. K. Murtazaev, JETP Lett. **101**, 714 (2015).

32. P. Peczak, A. M. Ferrenberg, and D. P. Landau, Phys. Rev. B **43**, 6087 (1991).

33. A. K. Murtazaev, M. K. Ramazanov, D. R. Kurbanova, M. K. Badiev, and Ya. K. Abuev, Phys. Solid State **59**, 1103 (2017).

34. M. Campostrini, M. Hasenbusch, A. Pelissetto, P. Rossi, and E. Vicari, Phys. Rev. B **65**, 144520 (2002).

Translated by Yu. Ryzhkov